Dyes and Pigments 99 (2013) 1016–1021

Contents lists available at ScienceDirect

Dyes and Pigments

journal homepage: www.elsevier.com/locate/dyepig

Solvent-dependent selective fluorescence assay of aluminum and gallium ions using julolidine-based probe

Jin Young Noh [a], Soojin Kim [b], In Hong Hwang [a], Ga Ye Lee [b], Juhye Kang [a], So Hyun Kim [b], Jisook Min [c], Sungsu Park [b], Cheal Kim [a,**], Jinheung Kim [b,*]

[a] Department of Fine Chemistry, Seoul National University of Science and Technology, Seoul, Republic of Korea
[b] Department of Chemistry and Nano Science, Global Top5 Research Program, Ewha Womans University, Seoul 120-750, Republic of Korea
[c] National Forensic Service, Seoul 158-707, Republic of Korea

ARTICLE INFO

Article history:
Received 22 June 2013
Received in revised form
28 July 2013
Accepted 29 July 2013
Available online 22 August 2013

Keywords:
Aluminum ions
Fluorescence chemosensor
Gallium ions
Julolidine
Turn-on sensor
Solvent dependence

ABSTRACT

The selective assay of aluminum and gallium ions is reported using fluorescence enhancement of a julolidine-based probe (PJI) in aqueous and nonaqueous solvents. The binding properties of PJI with metal ions were investigated by UV–vis, fluorescence, and electrospray ionization mass spectrometry. PJI gave no fluorescence in water, dimethylformamide, and methanol. The addition of aluminum ions switches on the fluorescence of the sensor PJI in both buffer and dimethylformamide, while other metal ions show no significant fluorescence changes. However, in methanol, its fluorescence can be selectively turned from a turn-on fluorescent sensor for gallium ions. The complex stability constants (K_a) for the respective stoichiometric 1:1 complexation of PJI with aluminium and gallium ions were obtained by fluorimetric titrations.

1. Introduction

The development of fluorescent sensors for selective detection of various biologically and environmentally relevant metal ions has been associated with an increasing interest in the potential impact of their toxic effects. Due to the widespread use of aluminum in food additives, aluminum-based pharmaceuticals, and cooking/storage utensils, human exposure to aluminum has increased. In addition, the frequent use of aluminum foil, vessels, and trays for convenience has moderately increased the possibility of aluminum inclusion in food. Long-term ingestion enables aluminum ions to spread throughout all tissues in humans and animals, and eventually accumulate in the bone. The iron binding protein is the main carrier of Al^{3+} in plasma. Aluminum ions can enter the brain and reach the placenta and fetus by the carrier. Aluminum ions may stay for an extended time in various organs and tissues before they are excreted through the urine. In addition, aluminum ions have been implicated as one of possible factors of Alzheimer's disease due to the accumulation of oxidative damage induced by the ions and may result in damage to the central nervous system in humans [1–4]. The sensitive bio-imaging of Al^{3+} in the cell will be essential for understanding the mechanism by which aluminum ions cause aluminum-induced human diseases, including Alzheimer's disease [2,3]. Thus, the development of selective detection and bio-imaging techniques of Al^{3+} is important to control the concentration levels in the biosphere and minimize the adverse effect on human health. Several types of small molecules have been examined for fluorescence Al^{3+} detection [5–16]. However, only a few of these probes has been utilized for imaging Al^{3+} in living cells.

Gallium is used in electronic devices, usually in the form of gallium arsenide. Gallium compounds are also used as possible diagnostic and antitumor agents. Aluminum and gallium have a very similar chemistry such as always having a +3 oxidation state. However, fluorescent chemosensors for gallium ions are even rare than those for aluminum ions, even though other techniques for trace gallium determination, such as ion exchange, adsorption, extraction, and atomic absorption spectrometry, have been developed. A few fluorescent chemosensors for Ga^{3+} detection have been reported, but their selectivity for Ga^{3+} towards Al^{3+} was very poor [17,18]. A need therefore remains for the development of

* Corresponding author. Department of Chemistry and Nano Science, Ewha Womans University, Seoul 120-750, Republic of Korea. Tel.: +82 2 3277 4453; fax: +82 2 3277 3419.
** Corresponding author.
E-mail addresses: chealkim@snust.ac.kr (C. Kim), jinheung@ewha.ac.kr (J. Kim).

0143-7208/$ – see front matter © 2013 Elsevier Ltd. All rights reserved.
http://dx.doi.org/10.1016/j.dyepig.2013.07.035

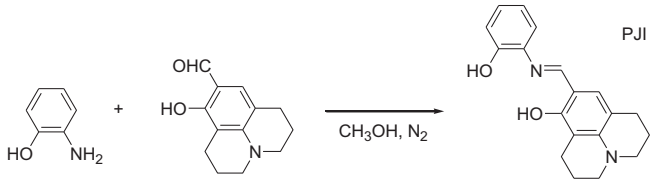

Scheme 1. Synthesis of the fluorescent sensor *ortho*-phenyljulolidineimine (PJI).

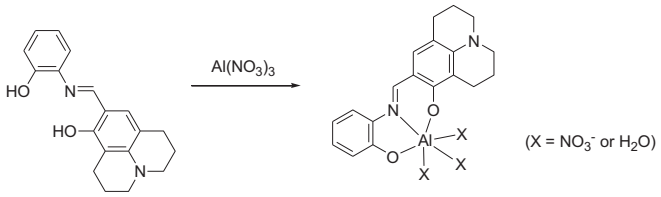

Scheme 2. Proposed structure of a 1:1 complex of PJI and Al^{3+}.

new and improved chemosensors for the selective determination of Ga^{3+}.

On the other hand, some molecular metal complexes containing Schiff base-type compounds are known to exhibit antitumor and antioxidative activities [19,20]. Schiff base organic ligands incorporating a fluorescent moiety have been used to assay specific metal ions. Although some Schiff base-type Al^{3+} chemosensors were recently reported [5–7,15–16], examples of water-soluble sensors that can be used for cell imaging and biological samples are rare. Chemosensors based on julolidine exhibit a selective sensing for Cu^{2+} and Fe^{3+} [21,22]. In this study, we report the metal-binding properties of another julolidine-based imine probe, which is the π-conjugated Schiff base receptor, and that exhibits enhanced fluorescence with high selectivity upon binding to Al^{3+} in water and dimethyl formamide (DMF), but to Ga^{3+} in CH_3OH. The possible application of the probe as an intracellular sensor of Al^{3+} is also reported by confocal fluorescence microscopy.

2. Results and discussion

The chemosensor, *ortho*-phenyljulolidineimine (PJI) was prepared using 8-hydroxyjulolidine-9-carboxaldehyde and 2-aminophenol with 72% yield (Scheme 1 and Supporting Information). To understand the binding properties of this PJI receptor towards various metal ions, such as Na^+, K^+, Ag^+, Ca^{2+}, Mg^{2+}, Ni^{2+}, Cd^{2+}, Mn^{2+}, Co^{2+}, Cu^{2+}, Zn^{2+}, Hg^{2+}, Pb^{2+}, Al^{3+}, Cr^{3+}, Fe^{3+}, Ga^{3+}, and In^{3+}, the fluorescence spectral response of the aqueous buffer (10 mM Tris–HCl pH = 7.0) solution of PJI was examined in the presence of each metal ion (Fig. 1a). Significant spectral changes were observed only in the case of Al^{3+}. The fluorescence intensity ratio (I_{Al}/I_{Ga}) of PJI measured in the presence of Al^{3+} and Ga^{3+} was 32, which was the highest relative to those reported with other chemosensors [5,6,15,23]. In contrast, treatment with other metal ions resulted in no significant changes, demonstrating that PJI is even highly selective for Al^{3+} over Ga^{3+} and In^{3+}.

The turn-on fluorescence response of PJI was observed for Al^{3+} with emission bands at 482 and 512 nm. Upon addition of Al^{3+}, the fluorescence intensity of PJI increased by 100-fold (fluorescence quantum yield $\Phi = 0.096$). The fluorescence spectral changes of PJI revealed the presence of an incremental amount of Al^{3+}. The fluorometric titration curve showed a steady and smooth increase with increasing Al^{3+} concentration, which demonstrated an efficient fluorescence response (Fig. 1b and Fig. S1a). The binding affinity of PJI towards Al^{3+} was quantified based on fluorescence titration experiments, affording the association constant (K_a) of 1×10^7 M^{-1} (Fig. S1b). Binding analysis using the Benesi-Hildebrand plot established that a 1:1 complex of PJI and Al^{3+} was responsible for the observed fluorescence enhancement

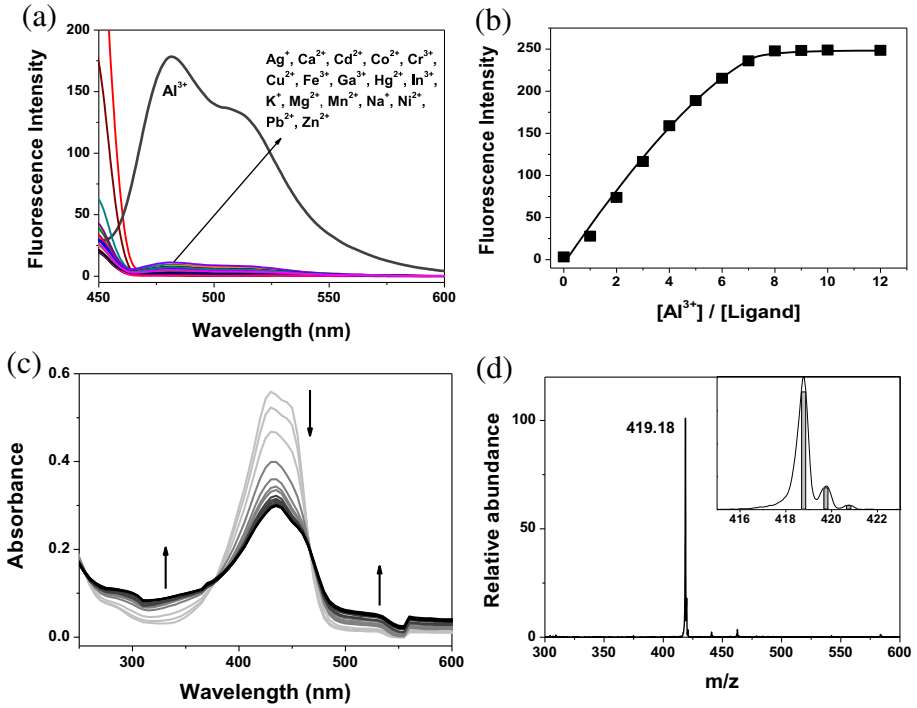

Fig. 1. (a) Emission spectra of PJI (0.5 μM) in the absence and presence of various metal ions (4.0 μM) using $E_\lambda = 450$ nm in 10 mM Tris buffer (pH = 7.0). (b) Fluorescence titration of PJI with Al^{3+} in aqueous solution. (c) UV–vis spectral changes of PJI (10 μM) as a function of the Al^{3+} concentration in 10 mM Tris buffer. (d) ESI-MS of PJI (1.0 μM) + Al^{3+} (1.0 μM) in Tris buffer (inset, Calculated isotope pattern represented by bars under the peak cluster). All fluorescence spectra were acquired in 10 mM Tris buffer with excitation at 450 nm at room temperature. A methanol stock solution of PJI was used for all experiments.

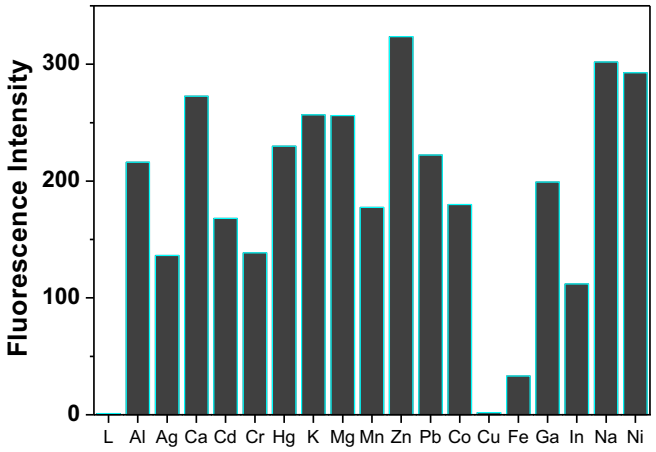

Fig. 2. Relative fluorescence of PJI and its complexation with Al^{3+} in the presence of various metal ions. The response of PJI was included as controls. Left to right: PJI alone (L corresponds to PJI) and PJI + Al^{3+} + M (M = Al^{3+}, Ag^{+}, Ca^{2+} Cd^{2+}, Cr^{3+}, Hg^{2+} K^{+}, Mg^{2+}, Mn^{2+} Zn^{2+}, Pb^{2+}, Co^{2+} Cu^{2+}, Fe^{3+}, Ga^{3+}, In^{3+}, Na^{+}, Ni^{2+}). Conditions: 0.5 μM PJI, 8 equiv Al^{3+}, and 8 equiv other metal ions (λ_{ex} = 450 nm).

(Scheme 2). Al^{3+} could be detected down to 0.13 μM based on the 3α/slope when 5 μM PJI was employed. In the pH dependence study of PJI-Al^{3+}, emission at 482 nm was only observed at pH 5.5–7.5 (Fig. 3, Fig. S2).

The absorption spectra of PJI changed upon addition of Al^{3+} ions (Fig. 1c). The band at 430 nm decreased without a marked shift and a weak UV band was observed around 300 nm. The presence of two clear isosbestic points for PJI supports the formation of a complex with only one stoichiometry (Fig. 3) .

The 1:1 complexation between PJI and Al^{3+} was also evidenced by using Job's plot and electrospray ionization mass (ESI-MS) spectral analysis. The positive mass spectrum exhibited one intense peak at m/z = 419 corresponding to the ion $[PJI - 2H^{+} + Al^{3+} + CH_3OH + 3H_2O]^{+}$ (Fig. 1d). The formulation of this ion was corroborated by isotope distribution patterns that matched the calculated pattern (Fig. 1d, inset). The ^{1}H NMR spectra of PJI recorded in nonprotic solvent upon addition of increasing Al^{3+} showed significant spectral changes (Fig. S3a). Two hydroxyl protons of PJI at 9.5 and 14.2 ppm progressively disappeared upon treatment with Al^{3+}, indicating that the OH protons were deprotonated upon complexation.

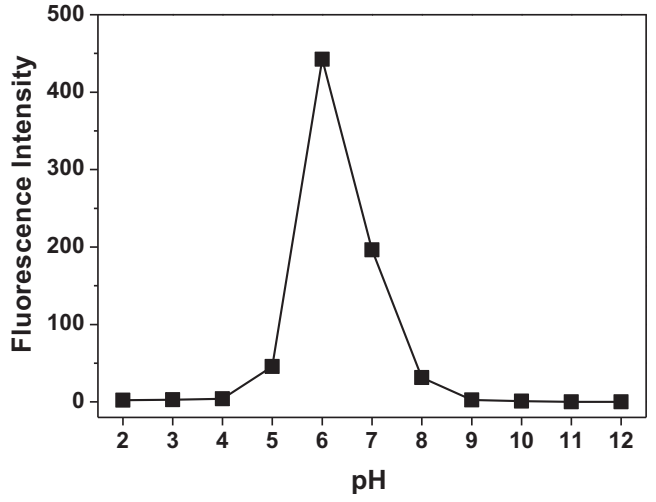

Fig. 3. pH dependence of the fluorescence intensity for solutions containing 0.5 μM PJI and 4.0 μM aluminum ions at 482 nm in 10 mM phosphate buffer.

The emission profiles of PJI (0.5 μM) or its Al^{3+}-bound form were unperturbed in the presence of 160 equiv of Na^{+}, K^{+}, Ca^{2+}, Mg^{2+}, Ni^{2+}, Cd^{2+}, Mn^{2+}, Zn^{2+}, and Hg^{2+} (Fig. 2). In addition, PJI was also selective over Ag^{+} at 16-fold excess and over Co^{2+}, Pb^{2+}, and Ga^{3+} at 8-fold excess. The fluorescence profiles of PJI were somewhat perturbed by In^{3+}, but PJI remained selective for Al^{3+} over In^{3+} at 2-fold excess.

In order to explore the fluorescence enhancement of PJI with Al^{3+} according to solvents, the fluorescence responses of PJI were examined in dimethylformamide (DMF) and methanol. The fluorescence response of PJI upon addition of Al^{3+} in DMF showed two similar emission bands at 493 and 520 nm, which were shifted due to solvent polarity relative to those observed in the buffer. PJI was also highly selective for Al^{3+} over competing metal ion analytes (Fig. 4a). Fluorescence enhancement upon treatment with Al^{3+} appeared as high as 400-fold (Fig. 4b).

When the fluorescence properties of PJI were examined in methanol, the selectivity for metal ions was changed unexpectedly. Fig. 5a shows the fluorescence spectra of PJI upon addition of metal ions in CH_3OH. Similar to the data in buffer and DMF, Al^{3+} enhanced the emission of PJI to some extent, while no significant changes of the fluorescence were observed with other competing metal ions. Interestingly, the addition of gallium ions changed the emission signals of PJI remarkably and the intensity was much greater than that of Al^{3+}. Upon addition of Ga^{3+}, the fluorescence intensity of PJI

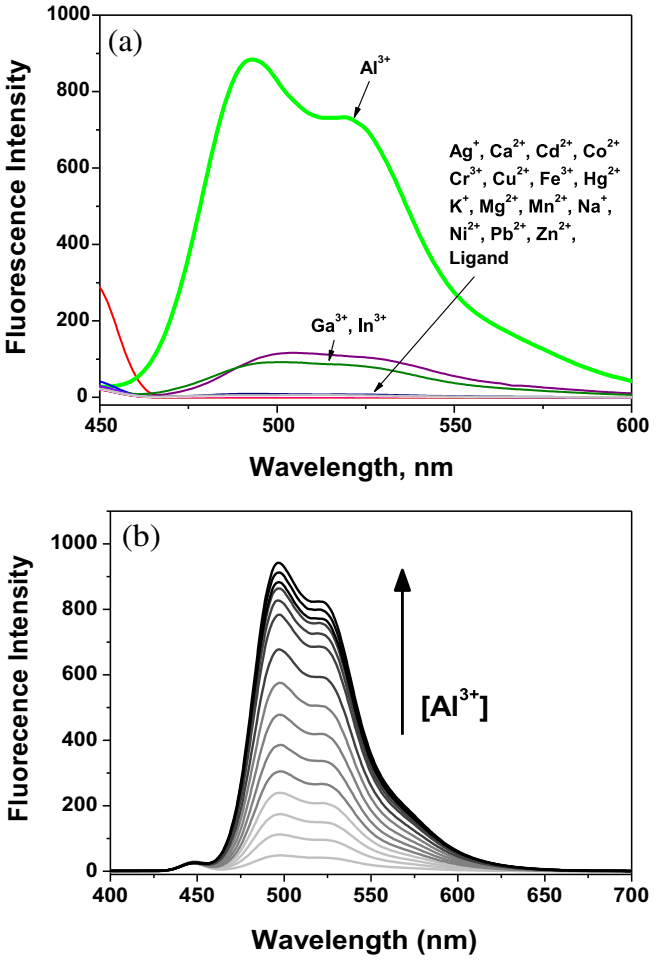

Fig. 4. (a) Emission spectra of PJI (2 μM) in the absence and presence of 10 equiv of various metal ions using E_{λ} = 450 nm in DMF. (b) Fluorescence response of PJI (2 μM) to Al^{3+} (0–4 μM) in DMF.

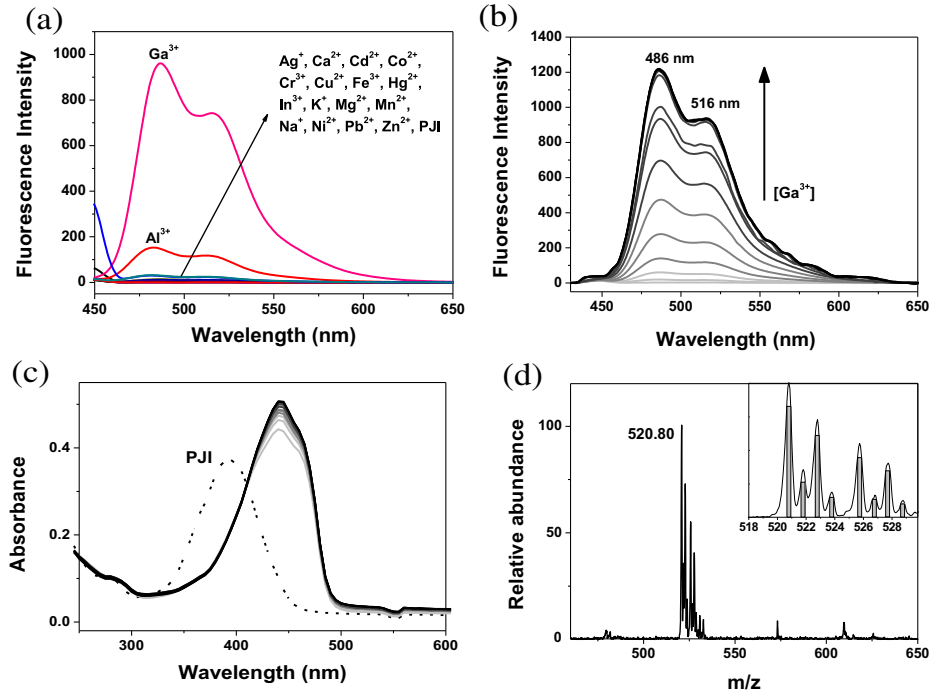

Fig. 5. (a) Emission spectra of PJI (2 μM) in the absence and presence of 7 equiv of various metal ions using $E_\lambda = 450$ nm in CH_3OH. (b) Fluorescence response of PJI (2 μM) to Ga^{3+} (0–18 μM) in CH_3OH. (c) Absorption spectral changes of PJI (10 μM) as a function of the Ga^{3+} concentration. (d) ESI-MS of PJI + Ga^{3+} in methanol (inset, Calculated isotope pattern represented by bars under the peak cluster). All experiments were performed using CH_3OH. All fluorescence spectra were acquired with excitation at 450 nm.

increased by 1400-fold ($\Phi = 0.152$) (Fig. 5b and Fig. S4). This turn-on response was accompanied by red shifts in emission (486 and 516 nm) maxima due to solvent polarity. The intensity ratio (I_{Ga}/I_{Al}) of PJI was 6.4, which is the highest relative to those reported with other fluorescence chemosensors [16]. The fluorescence titration of PJI afforded the association constant value $K_a = 2.5 \times 10^6$ M^{-1} (Fig. S5). The detection limit was 0.10 μM. The ^1H NMR spectra of PJI recorded in nonprotic solvent upon addition of gallium ions also showed a progressive disappearance of two OH protons (Fig. S3b).

The fluorescence responses of PJI were unperturbed by Na^+, K^+, Ag^+, Ca^{2+}, Mg^{2+}, Ni^{2+}, Cd^{2+}, Mn^{2+}, Co^{2+}, Cu^{2+}, Zn^{2+}, Hg^{2+}, Pb^{2+}, and Al^{3+} at 35-fold excess. Addition of more than 2 equiv In^{3+} resulted in almost half fluorescence intensity by Ga^{3+}. The UV–vis absorption changes upon addition of various concentrations of Ga^{3+} showed a bathochromic shift from 392 to 440 nm (Fig. 5c). A clear isosbestic point was observed at 410 nm.

These fluorescence spectra implied a structural change in PJI upon complexation with Ga^{3+}. To clarify the structural change upon complexation of PJI and Ga^{3+}, ESI-MS analyses were carried out. The ESI-MS results of a PJI + Ga^{3+} solution exhibited a positive ion at $m/z = 521$ corresponding to $[PJI - 2H^+ + Ga^{3+} + 4CH_3OH + H_2O]^+$ (Fig. 5d), the isotope distribution pattern of which is consistent with the formulation (Fig. 5d, inset). The ESI-MS results and Benesi-Hildebrand plot established a 1:1 binding stoichiometry for PJI- Ga^{3+}.

Then, we studied the bioimaging application of PJI for mapping aluminum ions in living cells. HeLa cells were first exposed to various concentrations (0–100 μM) of $Al(NO_3)_3$ for 5 h and then incubated with the chemosensor (5 μM) for 30 min. Low background fluorescence was observed in the cells (Fig. 6a) that had not been exposed to $Al(NO_3)_3$. The background fluorescence derived from cellular metal ions, such as Na^+, Ca^{2+}, Mg^{2+}, Zn^{2+}, etc, which also afforded low fluorescence with PJI (Fig. 1a). Weak but still discernible fluorescence was observed in the cells previously exposed $Al(NO_3)_3$ at 0.1 and 1 μM, compared to the unexposed cells. Strong fluorescence was observed in the cells previously exposed to $Al(NO_3)_3$ at 10 and 100 μM, as shown in Fig. 6a. Over fifty cells from the images of each treatment were randomly selected and the fluorescence intensities of individual cells were quantified using Image J program (Fig. 6b). Based on the mean fluorescence intensity data of cells, the cells exposed to the 0.1 μM Al^{3+} were discernible from the unexposed cells. These results indicate that the fluorescence intensities in the exposed cells depended on the $Al(NO_3)_3$ concentrations. The PJI chemosensor bound to intracellular Al^{3+} and emitted fluorescence, thus demonstrating its suitability for determining the exposure level of cells to aluminum ions.

3. Conclusions

We have described a unique fluorescent chemosensor PJI for aluminum and gallium and its solvent-dependent properties. PJI exhibited excellent selectivity for Al^{3+} and Ga^{3+} in different solvents over competing relevant metal ions and a large turn-on response for detecting these ions. Furthermore, PJI is capable of mapping aluminum levels in cells and this class of fluorophores might be exploited as specific and effective sensors for intracellular aluminum ions.

4. Experimental section

4.1. Materials and instrumentation

All solvents and reagents (analytical and spectroscopic grades) were obtained from Sigma–Aldrich (St. Louis, MO, USA) and used as received. Water was purified with a MilliQ purification system. The metal ion solutions were prepared with metal nitrate salts in methanol. NMR spectra were recorded on a Varian 400 spectrometer (Palo Alto, CA, USA). Chemical shifts (δ) are reported in ppm, relative to tetramethylsilane $Si(CH_3)_4$. Absorption spectra were

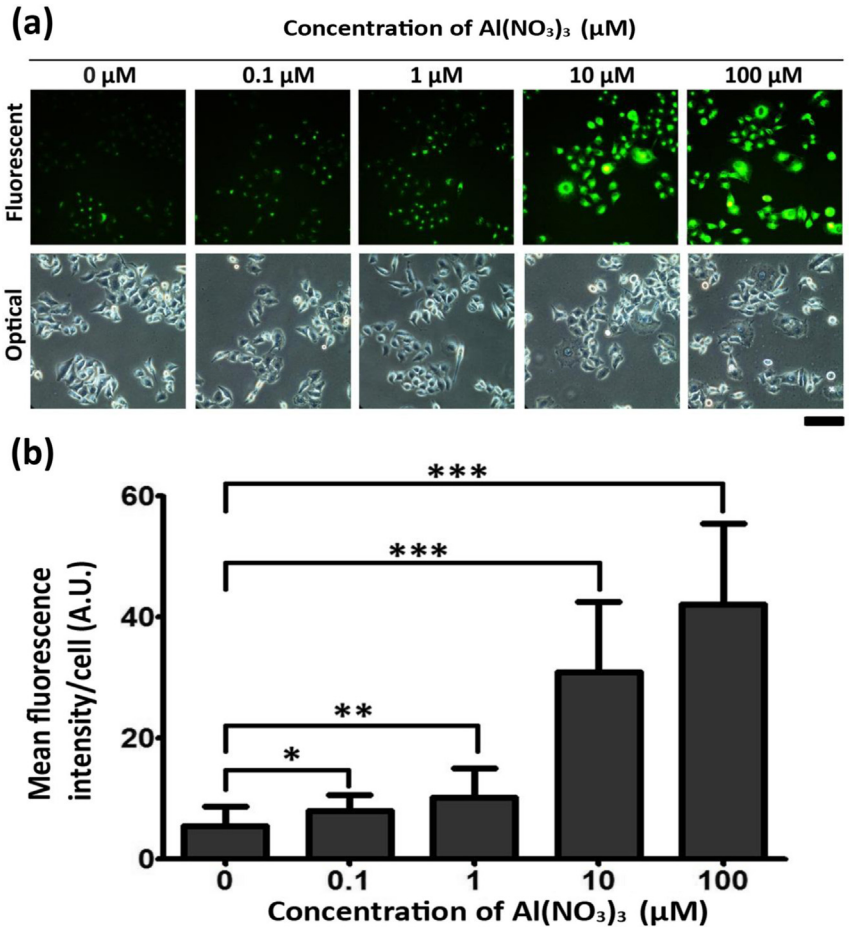

Fig. 6. (a) Observation of Al^{3+} in HeLa cells exposed to various concentrations (0–100 μM) of $Al(NO_3)_3$ for 5 h using the chemosensor (5 μM) and (b) the mean fluorescence intensities of cells from each treatment. The scale bar in the image indicates 50 μm. Over fifty cells from the images of each treatment were randomly selected and the fluorescence intensities of individual cells were quantified using Image J program. Graph data presentation: mean ± std (standard deviation). *p-value (t-test) < 0.0001, p-value (F-test) > 0.05. ** p-value (t-test) < 0.0001, p-value (F-test) < 0.05. *** p-value (t-test) < 0.0001, p-value (F-test) < 0.0001.

recorded at 25 °C using a Perkin–Elmer model Lambda 2S UV/Vis spectrometer (Waltham, MA, USA). Emission spectra were recorded on a Perkin–Elmer LS45 fluorescence spectrometer. Electrospray ionization mass spectra (ESI MS) of M^{3+}-PJI complexes were collected on a Thermo Finnigan (San Jose, CA, USA) LCQTM Advantage MAX quadrupole ion trap instrument, by infusing samples directly into the source at 25 μL/min using a syringe pump. The spray voltage was set at 4.7 kV and the capillary temperature at 70 °C.

4.2. Synthesis of ortho-phenyljulolidineimine (PJI)

2-aminophenol (0.55 g, 5 mmol) was mixed with 8-hydroxyjulolidine-9-carboxaldehyde (1.13 g, 5 mmol) in absolute methanol. The mixture was refluxed for 3 h under nitrogen. The solution was then cooled to room temperature and the solvent was evaporated. The brown product was recrystallized from methanol. The yield of PJI was 82% (1.26 g). ^{1}H NMR (methanol-d_4, 400 MHz) δ: 9.02 (s, 1H), 8.15 (d, 1H, J = 8.0 Hz), 7.71 (t, 1H, J = 7.6 Hz), 7.57 (m, 3H), 4.01 (m, 4H), 3.31 (m, 4H), 2.58 (m, 4H). ^{13}C NMR (DMSO-d_6, 100 MHz): δ 161.62, 157.91, 149.93, 146.79, 134.40, 129.59, 125.83, 119.61, 118.16, 116.12, 112.49, 108.44, 105.47, 49.42, 49.07, 26.79, 21.63, 20.66, 20.08. Calcd for $C_{19}H_{20}N_2O_2$ (308.37): C, 74.00; H, 6.54; N, 9.08%. Found: C, 74.25; H, 6.61; N, 9.21%. FAB MS m/z (M^+): calcd, 308.37; found, 308.39.

4.3. Fluorescence measurements

PJI was dissolved in methanol, and the PJI stock solution was diluted in water, DMF, or methanol to make the final concentration of 0.5 μM. Then, metal ions including $Al(NO_3)_3$ and $Ga(NO_3)_3$ was added to 3 mL of a chemosensor solution. After mixing, fluorescence spectra were obtained at room temperature.

4.4. Fluorescent imaging of intracellular Al^{3+} in cells

HeLa cells (CCL-2, ATCC, Manassas, VA, USA) were cultured in DMEM (Dulbecco's Modified Eagle Medium, Invitrogen, Carlsbad, CA, USA) supplemented with 100 units/ml Penicillin and Streptomycin (Invitrogen, Carlsbad, CA, USA), and 10% FBS (Fetal Bovine Serum, Invitrogen) in a humidified incubator at 37 °C with 5% CO_2. For fluorescent imaging of Al^{3+}, cells were seeded onto a 35 mm tissue culture plate at a density of 10^5 cells. $Al(NO_3)_3$ solutions were prepared by diluting10 mM $Al(NO_3)_3$ in 10 mM Bis-Tris (pH 7.1) with serum free DMEM. At 1 day after the seeding, the cells were treated with $Al(NO_3)_3$ at various concentrations (1–100 μM) for 5 h. After the treatment, the cells were three times washed with PBS containing 10 mM Bis-Tris. Then, they were incubated with 5 μM PJI chemosensor for 30 min at room temperature to stain intracellular Al^{3+}. The chemosensor (5 μM) has been prepared by diluting the chemosensor (10 mM) in methanol with PBS containing 10 mM Bis-

Tris. After staining, the cells were washed with PBS and microscopic images were taken using an inverted fluorescent microscope (TE2000-U, Nikon) equipped with a CCD camera (SPOT, Diagnostic Instruments, Inc., Sterling Heights, MI, USA). Over fifty cells from the images of each $Al(NO_3)_3$ treatment were randomly selected and the fluorescence intensities of individual cells were quantified using Image J program (NIH, USA). Statistical analysis was performed using GraphPad Prism Ver. 5 (GraphPad Software, Inc., La Jolla, CA, USA).

Acknowledgments

This work was supported by the National Research Foundation of Korea Grant funded by the Korea Government (2012008875, 2012001725, NRF-2013R1A2A2A03015101), the Converging Research Center Program through the National Research Foundation of Korea (NRF) funded by the Ministry of Education, Science and Technology (2011K000675), the National R&D program of the Ministry of Education, Science and Technology (MEST), Korea: Development of Molecular Sensing Technology (Code number 2012-009832), and BK21 (to S.K. and G.Y.L.).

Appendix A. Supplementary data

Supplementary data related to this article can be found at http://dx.doi.org/10.1016/j.dyepig.2013.07.035.

References

[1] Cronan C, Walker W, Bloom P. Predicting aqueous aluminium concentrations in natural waters. Nature 1986;324:140–3.
[2] Fasman G. Aluminum and alzheimer's disease: model studies. Coord Chem Rev 1996;149:125–65.
[3] Nayak P. Aluminum: impacts and disease. Environ Res 2002;89:101–15.
[4] Walton J. An aluminum-based rat model for alzheimer's disease exhibits oxidative damage, inhibition of PP2A activity, hyperphosphorylated tau, and granulovacuolar degeneration. J Inorg Biochem 2007;101:1275–84.
[5] Kim S, Noh JY, Kim KY, Kim JH, Kang HK, Nam SW, et al. Salicylimine-based fluorescent chemosensor for aluminum ions and application to bioimaging. Inorg Chem 2012;51:3597–602.
[6] Park HM, Oh BN, Kim JH, Qiong W, Hwang IH, Jung KD, et al. Fluorescent chemosensor based-on naphthol–quinoline for selective detection of aluminum ions. Tetrahedron Lett 2011;52:5581–4.
[7] Sen S, Mukherjee T, Chattopadhyay B, Moirangthem A, Basu A, Marek J, et al. A water soluble Al^{3+} selective colorimetric and fluorescent turn-on chemosensor and its application in living cell imaging. Analyst 2012;137:3975–81.
[8] Kim SH, Choi HS, Kim J, Lee SJ, Quang DT, Kim JS. Novel optical/electrochemical selective 1,2,3-triazole ring-appended chemosensor for the Al^{3+} ion. Org Lett 2010;12:560–3.
[9] Arduini M, Felluga F, Mancin F, Rossi P, Tecilla P, Tonellato U, et al. Aluminium fluorescence detection with a FRET amplified chemosensor. Chem Commun 2003;13:1606–7.
[10] Maity D, Govindaraju T. Conformationally constrained (Coumarin–-Triazolyl–Bipyridyl) click fluoroionophore as a selective Al^{3+} sensor. Inorg Chem 2010;49:7229–31.
[11] Maity D, Govindaraju T. Pyrrolidine constrained bipyridyl-dansyl click fluoroionophore as selective Al^{3+} sensor. Chem Commun 2010;46:4499–501.
[12] Maity D, Govindaraju T. A differentially selective sensor with fluorescence turn-on response to Zn^{2+} and dual-mode ratiometric response to Al^{3+} in aqueous media. Chem Commun 2012;48:1039–41.
[13] Hau F, He X, Lam WH, Yam V. A selective and ratiometric bifunctional fluorescent probe for Al^{3+} ion and proton. Chem Commun 2011;47:8778–80.
[14] Wang YW, Yu MX, Yu YH, Bai Z, Shen Z, Li FY, et al. A colorimetric and fluorescent turn-on chemosensor for Al^{3+} and its application in bioimaging. Tetrahedron Lett 2009;50:6169–72.
[15] Lee J, Kim H, Kim S, Noh JY, Song EJ, Kim C, et al. Fluorescent dye containing phenol-pyridyl for selective detection of aluminum ions. Dyes Pigm 2013;96:590–4.
[16] Maity D, Govindaraju T. Naphthaldehyde–urea/thiourea conjugates as turn-on fluorescent probes for Al^{3+} based on restricted C= N isomerization. Eur J Inorg Chem 2011;36:5479–85.
[17] Kimura J, Yamada H, Orura H, Yajima T, Fukushima T. Development of a fluorescent chelating ligand for gallium ion having a quinazoline structure with two schiff base moieties. Anal Chim Acta 2009;635:207–13.
[18] Kimura J, Yamada H, Yajima T, Fukushima T. Enhancement effect of some phosphorylated compounds on fluorescence of quinazoline-based chelating ligand complexed with gallium ion. J Luminescence 2009;129:1362–5.
[19] Padhye S, Kauffman G. Transition metal complexes of semicarbazones and thiosemicarbazones. Coord Chem Rev 1985;63:127–60.
[20] Silveira VC, Luz J, Oliveira C, Graziani I, Ciriolo M, Ferreira A. Double-strand DNA cleavage induced by oxindole-Schiff base copper(II) complexes with potential antitumor activity. J Inorg Biochem 2008;102:1090–103.
[21] Maity D, Manna A, Karthigeyan D, Kundu T, Pati S, Govindaraju T. Visible–near-infrared and fluorescent copper sensors based on julolidine conjugates: selective detection and fluorescence imaging in living cells. Chem Eur J 2011;17:11152–61.
[22] Narayanaswamy N, Govindaraju T. Aldazine-based colorimetric sensors for Cu^{2+} and Fe^{3+}. Sen Actuators B Chem 2012;161:304–10.
[23] Sun X, Wang YW, Peng Y. A selective and ratiometric bifunctional fluorescent probe for Al^{3+} ion and proton. Org Lett 2012;14:3420–3.